

## TOWARDS THE AUTOMATIC DETECTION OF GEOSPATIAL CHANGES BASED ON DIGITAL ELEVATION MODELS PRODUCED BY UAV IMAGERY

T. Bauman, O. Almog, S. Dalyot

Mapping and Geo-Information Engineering, Civil and Environmental Engineering Faculty, The Technion, Israel  
- (talbauman, almogo, dalyot)@technion.ac.il

### ICWG II/III: Pattern Analysis in Remote Sensing

#### KEYWORDS:

Change detection, UAV, DEM, Multi-resolution analysis

#### ABSTRACT:

Reliable and accurate geospatial-databases (Digital Elevation Models, DEMs) are an essential component of Geographic Information Systems (GIS). One of their most important uses is change detection - an invaluable tool for environmental interpretation and evidence-based action. High-performance and inexpensive Unmanned Aerial Vehicles (UAVs) are increasingly used for the acquisition of timely geospatial information (imagery) for the production of DEMs for geospatial change detection. DEMs produced from UAV imagery have very high resolution and very good internal accuracy. However, their absolute location accuracy is inferior to other mapping technologies. Therefore, existing change detection methods, which are based on the point-by-point comparison, will perform poorly when processing DEMs created from UAV imagery since they are limited in reliably separating real physical changes from artifacts related to DEM inherent inaccuracy or errors. This paper presents a novel methodology that overcomes these deficiencies, by implementing a hierarchical analysis and modeling process, in which a sequence of methods is used to automatically identify and match unique homological features, such as building corners or topographic maxima, in the various height models. These provide geospatial anchors that bring out local geospatial discrepancies between the models. Those are then used to "repair" (align) the models to the same geospatial reference system, at which point change-detection is performed. Experimental results showed that when calculating point-by-point height differences, 98.99% of the area was falsely classified as changed, whereas implementing our method adequately detected all the actual changes in the area with no false positives, correctly classifying 0.16% of the area as changed.

### 1. BACKGROUND

Change detection is an invaluable tool for environmental interpretation and evidence-based action, commonly implemented in GIS systems while relying on Digital Elevation Models (DEMs) that serve as a reliable representation. Change detection mostly requires a spatial adjustment of the DEMs to retrieve accurate results. Commonly used spatial adjustment processes of geospatial databases are based on points of interest, and are usually consists of two main stages: (1) the determination of homological features (coupling objects that describe the same physical phenomenon in the various databases); (2) the determination of the most suitable spatial transformation between the databases, such that it minimizes the spatial difference that exists after the transformation. In the second stage of the process, the calculation of single and uniform (global) conversion parameters between the various databases is usually performed - an assumption that is not always justified due to the differences of the databases. The use of single and uniform spatial transformation may impair the quality and accuracy of the data obtained after completion of the process, i.e. extraction and identification of inaccurate and unreliable changes. Different phenomena such as raw data, production processes, differences in reference systems, resolution, etc., affect the representation of different objects in the area, so that when a particular feature is compared in two different databases, a uniform global mismatch will sometimes occur. Therefore, there is a need for local, rather than global, analysis, in order to find an optimal solution of spatial transformation between the various databases, i.e. creating a set of regional (or local) transformations that ensures continuity and data representation.

The comparison mechanism must base on the topological structure of the data (Heipke 2014, Ben-Haim et al., 2014). If the existing gaps are untreated and minimized prior to the comparison process, they greatly affect data reliability, especially for processes such as change detection (Wang and Wade, 2008). Most of the studies that attempt to deal with the problem make use of global spatial adaptations carried out manually, while ignoring local reciprocal interactions (Podobnikar, 2005; Choussiafis et al., 2012). Another example can be found in Papasaika et al. (2009, 2011), which attempted to address the problem by diluting the representation (e.g., slope, roughness, and appearance) for the global adjustment.

Ben-Haim et al. (2012) attempted to find a single and uniform transformation between two geospatial databases, and found that there are local trends in the flat attribution of the various objects, which changes according to the location of the area in the database, hence the necessity of analyzing regional trends and finding a set of local adaptations for more accurate and reliable geospatial analyzes. The authors chose to represent local suitability by dividing the databases in a hierarchical way into quarters. Most of the geospatial databases behave arbitrarily, which is less similar to fixed quarters and more to patches with different coverage, so there is a need to examine the results of Ben-Haim et al. (2012), given the distribution of a different irregular and permanent area for each database or infrastructure (Zhao et al., 2013). Further studies have shown that in order to obtain more accurate results in the index of the correct fit of the topology and geometry presented, while minimizing existing spatial differences, it is necessary to first anchor and process spatial matching between the data repositories, e.g., from the fusion of several databases (Safra and Doytsher, 2006, Sester et

al., 2014, Hebel et al. 2013), or based on homological points of interest that describe consistent and prominent entities in data (such as endpoints in topography (Dalyot, 2010).

This study focuses on the development of a methodology based on multi-resolution analysis of DEMs, with the goal of retrieving optimal spatial transformation – or a set of such, which will enable accurate quantification of the changes that occurred in the field, while maximizing the neutralization of contradictions that are not part of the changes. The first stage will rely on finding and matching homological points between the various databases, which are characterized by uniform trends in their flat attribution. These will enable the second phase of the extraction of spatially compatible regions locally, thereby ensuring the flexibility of spatial matching and maintaining continuity, allowing for more accurate and reliable detection of changes. In this way, it will be possible for each local area in database A to adopt a spatial transformation to the homological zone in database B, in order to achieve maximum spatial compatibility between the databases, which will maintain continuity in the presentation of data.

As a result of the proliferation of modern technologies for the production of DEMs, models are being produced that present a different level of detail, coverage, resolution and accuracy. As a result, DEMs produced in different technologies, at different purchasing conditions and at different times, will almost always present different and changing data and qualities. These will result in a different presentation of the physical phenomena observed in the area (hill, structure, shed, wall) in the various models, which cause the location and shape of the phenomenon to be different, sometimes in a significant manner (Fig. 1). Some of the differences in the description are derived from changes in the field between the various acquisition times, but a large part is derived from the differences in internal definitions of the models, such as datum, precision, resolution, level of detail, as well as inherent inaccuracies. As a result, automatic detection of changes, based on various DEMs, may yield partial insights at best - and errors at worst.

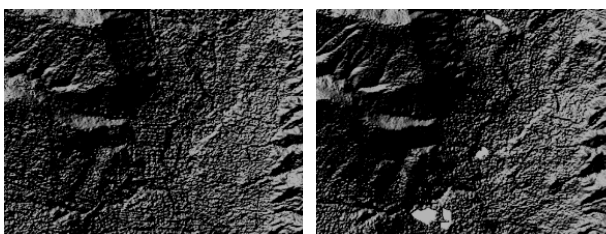


Figure 1. Shaded relief representation of two DEMs of the same area, produced by different technologies and at different times: gaps in the representation of the relief of physical phenomena in location, both in height and in detail.

The need to use innovative mapping technologies, such as UAVs, to produce detailed and precise DEMs is sharpened under conditions of work in densely built and densely populated areas. A UAV is now a relatively simple technological solution, enabling relatively short time and relatively simple operation complexity to produce a DEM from the images, to obtain an up-to-date and reliable snapshot (Kršák et al., 2016). However, although the internal accuracy of the model produced is high, the external accuracy is still relatively low, since most of the UAVs use location measurement using a low accuracy GNSS (error of several meters at best). Tuttas (2017) addressed the external accuracy problem using photogrammetric control points on the ground. Although this solution provides an accurate change detection, it requires advanced measuring instruments which

makes the use of UAV a much more expensive. Thus, without using photogrammetric control points, if a quantitative comparison of the changes that occurred in the field between different times from a DEM produced by a UAV to an existing DEM is likely to produce erroneous and inaccurate results. The inherent differences and inaccuracies of the various DEMs (resolution, datum, information acquisition technique, etc.) add uncertainty about the quality of the solution. Therefore, the basis for this research is the development of advanced automatic algorithms and methodologies, aimed at minimizing spatial gaps. These methods can also be used to identify and quantify in an informed and optimal manner physical changes that occurred in the field between different times. The ability to distinguish the signal from noise, will enable correct decision making, and the ability to analyze reliably for various geospatial analysis processes.

One of the innovative methodologies developed for dealing with databases comparison is Multi-Resolution Analysis, which uses unique geospatial characteristics by down-sampling database resolution at different stages and finding the change between stages. Date et al. (2001), for example, used Multi-Resolution Analysis to enable inclusion in favor of a three-dimensional computer graphic display efficiently using Orthophoto and DEM. One of the main problems in this use is the multiplicity of details and information (since in order to simulate reality optimally, use as much information and resolution as possible). A multiplicity of information causes slow computational power operations, thereby damaging the computerized 3D product. In order to solve this problem, it is necessary to reduce the information in a way that does not harm information or connectivity. The authors used a HAAR transformation for the DEM, and converted h-disk wavelet to Orthophoto processing. In this way, they were able to find the most appropriate generalization for the three-dimensional graphic representation of the database in an efficient manner.

Using Multi-Resolution Analysis of geospatial databases, spatial phenomena can be automatically detected in the database. Falkowski et al. (2006) developed a methodology for automatic extraction of vegetation from DSM (Digital Surface Model), produced using LiDAR (Light Detection And Ranging). The use of multi-resolution analysis on DSM enabled the authors to search for a spatial phenomenon (by tree radius, tree scale, and curvature) at varying resolutions, thus limiting the search to a specific shape and/or size. When we try to find homological points for the sake of calculating the spatial localization between two geospatial databases, we can also use Multi-Resolution Analysis, as Falkowski et al. (2006), and extend the search in the database for various resolutions to evaluate the quality of the interest points' extraction. The use of image processing tools for DEMs is an innovative technique that can be used to analyze three-dimensional databases, such as point clouds, which are now a common product of laser-based mapping as well as UAV-based photogrammetry.

## 2. METHODOLOGY

The methodology in this research is based on three main stages: (1) interest point detection and matching, (2) spatial adjustment, and (3) change detection with noise filtering. For identifying homological interest points, computer image processing methodologies are used. In the spatial adjustment phase, a local comparison is performed by dividing the databases to triangles and matching between the databases locally and independently.

## 2.1 Interest Points Detection and Matching

The first step in the process of identifying changes is matching the DEM databases. If it is not possible to adequately compare the databases, it will be difficult to differentiate between the actual changes and inherent global and local discrepancies and noise. An example is given in Fig. 2, where the discrepancy between two databases cannot be solved by moving one database to the other. In Fig. 2, red can be seen as a negative change in height (a drop-in height) and a green change in positive height (height increase). It is clear that the size and direction of the horizontal discrepancy to be performed prior to calculation, depicted as vectors, is not uniform and varies, where the lower part depicts larger discrepancies when compared to the upper part.



Figure 2. Example of the calculation of height difference performed without spatial adjustment: areas are wrongly classified as a change in the area (red and green).

Since the DEM produced by UAV is analogous to a database that is uniform in density and having a very high resolution, thus it is similar to an image, we decided to use image processing tools for point detection. In image processing, a large number of algorithms for the automatic identification of objects in images exists. One of the advanced object recognition algorithms is the Scale-Invariant Feature Transform (SIFT) (Lowe, 1999). The SIFT algorithm uses a multi-resolution analysis of images. This type of analysis is performed by reducing the resolution of the image and comparing the variable resolutions. After down-sampling the resolution, the objects that remain in the image are objects that are irregularly different from their environment. After repeating the resolution down-sampling step several times, interest points can be located in the image. The algorithm performs these actions for each individual image and then looks for a match between homological interest points in each image.

Another method for finding homological points using multi-resolution analysis uses the Gaussian filter (Lowe, 2004). This method is performed by using the Gaussian filter on the image, and from here the missing image is subtracted from the original image. This method makes extensive use of image processing problems. For identifying the edges, the use of the Gaussian filter is a significant and necessary component (Sharifi et al. 2002). The main challenge in locating edges is to extract the edges only with no additional noise, and the ability to separate the noise from the edges is limited, the only option is to set a Threshold value in advance. The threshold value can reduce the incorrect identification of edges, although it can reduce the precision and hermetic of the process.

After detecting homological points using SIFT, we have found that SIFT incorrectly matches some of the points, although we used only the high score homological points. Accordingly,

implemented a filtering algorithm to detect the incorrectly matched points by calculating the average, median, and standard deviation of the set to remove these errors. An example is depicted in Fig. 3.

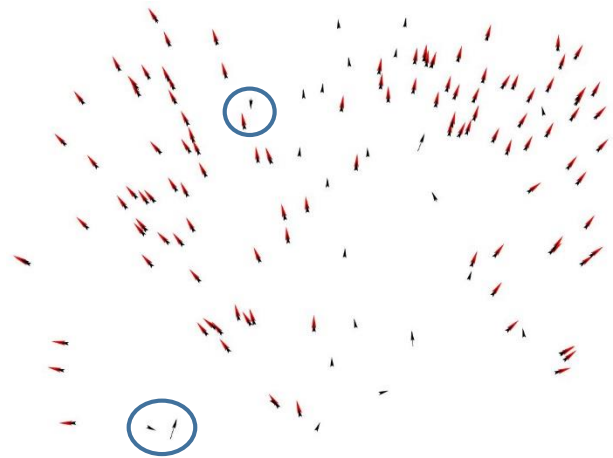


Figure 3. Vectors depicting the spatial matching of the homological points: before filtering (black), and after filtering (red); homological points that are filtered (blue circle).

## 2.2 Spatial Adjustment

In this study, we examined a different distribution of data, which is not arbitrary as the global transformation, and is directly related to the quantity and distribution of the homological points. The most basic form of dividing space into cells by points is triangulation. This we do based on the homological points using the Delaunay triangulation. This way, each DEM is divided into local triangular areas (sections), which are based on the homological points' structure, receiving a structure of homological triangles that should spatially correspond.

## 2.3 Change Detection with Noise Filtering

Once we have divided the databases into small sections using the Delaunay triangles, we perform local change detection on every triangle. We compute the transformation from the second database to the first for each triangle separately. To assess this stage, we have used two transformation models: (1) Affine transformation, and (2) Inverse Distance Weighting (IDW).

### 2.3.1 Affine Transformation

For affine transformation it is necessary to find the 6 parameters for each triangle:

$$\begin{aligned} x' &= a + cx + dy \\ y' &= b + ex + fy \end{aligned} \quad (1)$$

The six transformation parameters (a, b, c, d, e, f) are calculated using the least squares adjustment, where (x, y) are the coordinates of the vertices forming the triangle from the second database, and (x', y') are the coordinates of the vertices forming triangle from the first database. This is solved for each triangle, giving six equations for calculating the six transformation parameters (zero-degree of freedom). The partial derivative matrix A is considered directly from the equation of the characteristic transformation:

$$A = \begin{bmatrix} 1 & 0 & x_1 & y_1 & 0 & 0 \\ 0 & 1 & 0 & 0 & x_1 & y_1 \\ \vdots & \vdots & \vdots & \vdots & \vdots & \vdots \\ 1 & 0 & x_n & y_n & 0 & 0 \\ 0 & 1 & 0 & 0 & x_n & y_n \end{bmatrix}_{(n \times 6)} \quad (2)$$

Vector L is the measurement vector with the coordinate values of the second triangle:

$$L = \begin{bmatrix} x'_1 \\ y'_1 \\ \vdots \\ x'_n \\ y'_n \end{bmatrix}_{(n \times 1)} \quad (3)$$

The affine transformation parameters (a, b, c, d, e, f) are obtained after calculating the solution vector (X):

$$X_{(6 \times 1)} = (A^T A)^{-1} (A^T L) \quad (4)$$

### 2.3.2 IDW

In order to calculate the transformation using IDW, first we calculate the differences between the homological coordinates of each pair of triangles (based on their homological vertices):

$$\begin{bmatrix} dx_1 \\ dy_1 \\ dz_1 \end{bmatrix} = \begin{bmatrix} x_1 - x'_1 \\ y_1 - y'_1 \\ z_1 - z'_1 \end{bmatrix} \quad (5)$$

$$\begin{bmatrix} dx_2 \\ dy_2 \\ dz_2 \end{bmatrix} = \begin{bmatrix} x_2 - x'_2 \\ y_2 - y'_2 \\ z_2 - z'_2 \end{bmatrix}$$

$$\begin{bmatrix} dx_3 \\ dy_3 \\ dz_3 \end{bmatrix} = \begin{bmatrix} x_3 - x'_3 \\ y_3 - y'_3 \\ z_3 - z'_3 \end{bmatrix}$$

The differences (dx, dy, dz) between the homological points are the parameters for the IDW transformation. Depicted in Fig. 4, every triangle vertex has a corresponding spatial translation (dx<sub>i</sub>, dy<sub>i</sub>, dz<sub>i</sub>), thus every point inside the triangle is influenced by these values according to the distance from them, as described in Equations 6 and 7.

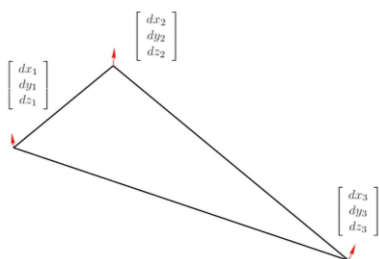


Figure 4. Each vertex of the triangle represents two homological points in the databases, while the red arrow shows the difference vector in size and direction, between the databases.

Now for each point (x, y) within the first triangle, the horizontal distances,  $l_i$ , where  $i=1:3$ , to all triangle corners are calculated, depicted in Equation 6.

$$l_1 = \sqrt{(x - x_1)^2 + (y - y_1)^2}$$

$$l_2 = \sqrt{(x - x_2)^2 + (y - y_2)^2} \quad (6)$$

$$l_3 = \sqrt{(x - x_3)^2 + (y - y_3)^2}$$

Based on the distances, the transformation parameters for each point in the triangle from the second database will be carried out according to Equation 7.

$$x' = x + \frac{\sum_{i=1}^3 l_i dx_i}{\sum_{i=1}^3 l_i}$$

$$y' = y + \frac{\sum_{i=1}^3 l_i dy_i}{\sum_{i=1}^3 l_i} \quad (7)$$

$$z' = z + \frac{\sum_{i=1}^3 l_i dz_i}{\sum_{i=1}^3 l_i}$$

Now that the transformation is calculated for a specific point (whether via IDW or affine transformation), we can transform each triangle, composed of all database points that fall inside it, in the second database to the corresponding triangle in the first database. An example of the data structure is depicted in Fig. 4. If required, it is also possible to filter triangles that are considered as noise to the system, e.g., triangles that are very small in area or have an irregular geometry. For example, we measured the angle of each “shift vector” in the triangle (every triangle contains 3 “shift vectors” from the second database to the first database), as shown in Fig. 4.

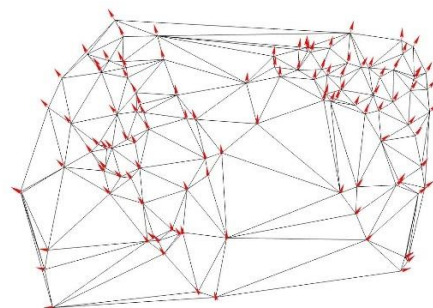


Figure 4. Delaunay triangulation based on homological points. The “translation vector” representing the local shift between the databases for each vertex is represented by a red arrow.

### 3. EXPERIMENTAL RESULTS

The experiments in this study were carried out in open urban and desert areas, where the DEMs were produced using Pix4D on images collected by an off-the-shelf consumer level UAV DJI Phantom 4 Advanced. To evaluate the reliability and potential of implementing SIFT on a DEM data structure, we first compared its results to the ones received using an Orthophoto database, with the results depicted Fig. 5. For the urban area, 300 images were taken, producing a database covering approximately 0.05 sq

km. The same area was scanned twice with a time difference of 57 days. For the data generated we produced an orthophoto and a DEM, both with a resolution of 0.25 m. For the Orthophoto, only 26 homological points are identified and coupled, whereas for the DEM produced for the same area, 212 homological points are identified and coupled. Above from the sheer volume of the number of homological points, we can see that the distribution of points is much wider and dispersed when we compare the results of the DEM to those of the orthophoto. These results show that while the orthophoto can be largely influenced by the existing environmental and production conditions, thus affecting the results of point identification, the DEM is much less influenced by these. In Fig. we can see that different lighting conditions exist: in the first database (right) there is almost no shadow, whereas in the second database (left), the extent of the shadow is much more evident. These results are very promising, proving that implementing image processing tools on a DEM can produce qualitative results for point detection, where the large number and dispersion of homological points make it possible to implement the local adjustment and transformation.

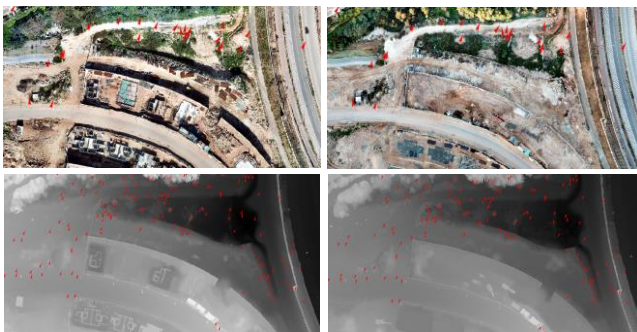


Figure 5. Point identification in the two databases: orthophoto (top) and DEM (bottom) representation, 26 and 212 homological points, respectively.

After the homological points are identified, we calculate several transformations to evaluate our approach. First, we calculate a global affine transformation between the two databases that relies on all homological points, where one database is transformed into the other, and height changes are calculated per DEM point. The results of this process are depicted in Fig. 6, where height changes above half a meter are represented in green, and height changes below half a meter are represented in red. Although some actual changes can be identified, as the building walls in the bottom of the figure, there are still many parts marked falsely as change; for example, the road area on the right that has not changed between the two databases. This incorrect change detection quantification is the clear result of non-uniform transformation between the two databases that cannot be quantified by a single global affine transformation.

We then evaluated the change detection based on local analysis, according to the proposed Delaunay triangulation, depicted in Fig. 7. For each triangle, we separately calculate the 6 local transformation parameters from the second database to the first. We then perform the transformation for each triangle independently to quantify the changes.

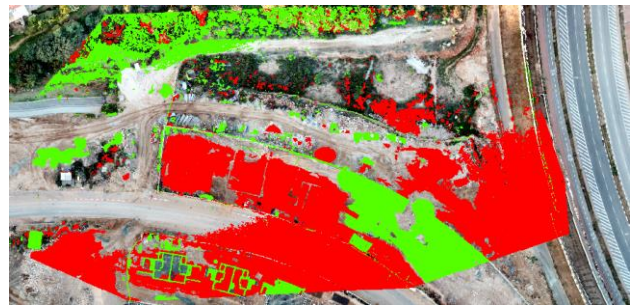


Figure 6. Identification of changes by the subtraction of the DEMs after global affine transformation: above half a meter change (green), and below half a meter change (red).



Figure 7. Delaunay triangulation based on 212 homologous points superimposed on the DEM.

Fig. 8 depicts the change detection results. Evident changes are visible in the construction area, but as opposed to the global transformation, there are no false-positive changes (for example, in the road area). While the global transformation makes use of all the points simultaneously, so that the transformation parameters are affected by errors from all of the set distributing local trends on all data, the local transformation uses each triangle separately, not affected by discrepancies derived from distant points (correct or not).

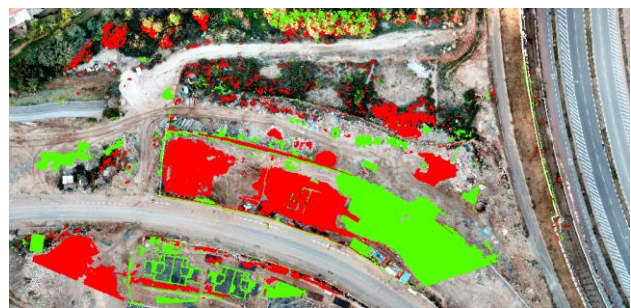


Figure 8. Identification of changes by the subtraction of DEMs after local affine transformation Increase in height above half a meter (green) Drop in height above half a meter (red).

To further validate our results, we calculate false positive and false negative error statistics according to five height comparisons, depicted in Table 1: (1) “direct” comparison that relies on the original database coordinates; (2) average shifting, moving one database to the other by calculating the average of the differences (3D translations) of the homological points; (3) global affine transformation of the database using the homologous points; (4) localized affine transformation for each triangle separately; and, (5) localized IDW transformation for each triangle separately. Values show that while the global

processes produce inaccurate change detection results, the local affine and IDW processes produce much better results, accurately identifying spatial changes that occurred.

Comparison Model	False positive (%)	False negative (%)
Direct	32	43
Global average shifting	12	31
Global affine	12	35
Local affine	0	9
Local IDW	1	9

Table 1. Comparison of false positive and false negative errors using all five models in an urban area.

For the desert area, 450 images were taken, producing a database covering approximately 0.02 sq km. The same area was scanned twice with a time difference of 1 hour. For the data generated we produced a DEM in a resolution of 0.25 m. After the first scan, we physically made several small morphological changes in the topography, before conducting the second scan, such that a change detection analysis should show that most of the area did not change. The topographies before and after are depicted in Fig. 9. The time difference between the two missions was less than one hour.

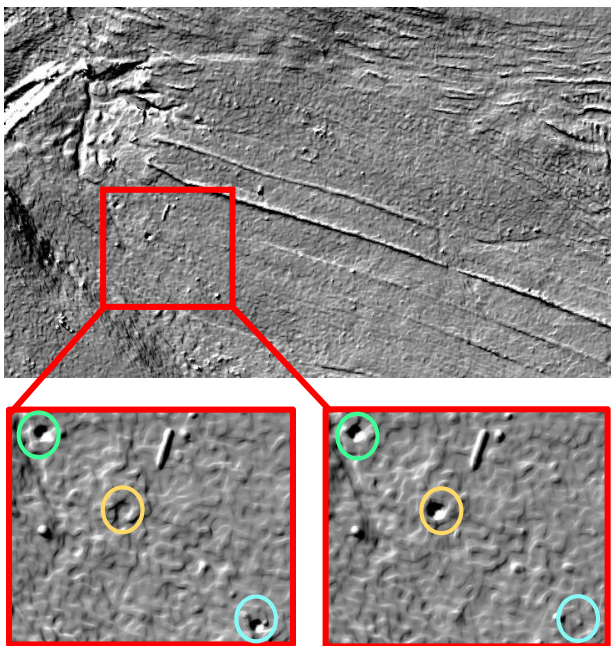


Figure 9. Shaded relief representation of the two DEMs with a zoomed are: before (right) 2 holes (green and orange) and flat land (blue), and after (left) 2 holes (green and blue) and covered hole (orange).

Figure 10 depicts the results of the global affine transformation of the two databases. Although the middle area shows good alignment of the two databases, both sides show an erroneously classified change detection area. Figure 11 depicts the results achieved after implementing the approach presented here, clearly showing that the two changed holes were correctly identified, with almost no false positives.

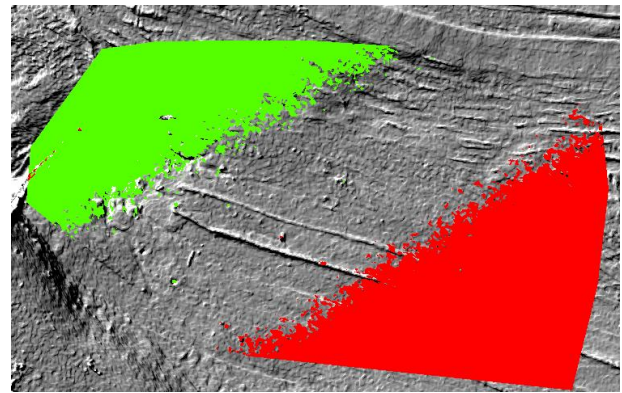


Figure 10. Identification of changes by the subtraction of DEMs after a global affine transformation: above 5 cm change (green), and below 5 cm change (red).

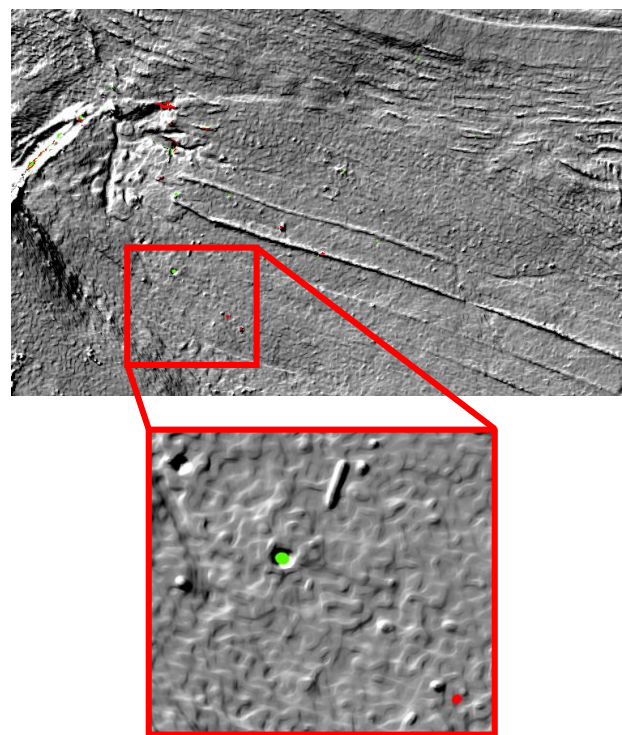


Figure 11. Identification of changes by the subtraction of DEMs after local affine transformation Increase in height above 5cm (green) Drop in height above 5cm (red).

Table 2 depicts the calculated false positive error statistics according to the five height comparisons (similar to Table 2). Only the local transformations did not identify false positive errors, allowing reliable change detection.

Comparison Model	False Positive (%)
Direct	99
Global average shifting	47
Global affine	49
Local affine	0
Local IDW	0

Table 2. Comparison of false positive errors using all five models in a desert area.

#### 4. DISCUSSION

Our approach provides a novel methodology for the detection of geospatial changes based on location-dependent multi-resolution analysis of DEMs produced by off-the-shelf consumer level UAV imagery. By implementing the automatic processes, we succeeded in accurately detecting topographical changes as small as 18 cm in diameter and 10 cm in depth with no false positives. More broadly, this research introduces a new approach to change detection from DEMs using image processing and feature matching techniques from the domain of image analysis. Moreover, the fully automatic implementation obviates the need for manual preprocessing or the use of ground control points.

Our research allows any simple user with a UAV and appropriate processing software to generate change mapping without control points or preliminary matching between the different databases. The local analysis we performed in the study assists in the process of identifying changes and eliminates the effect of errors in databases that are caused by environmental conditions and/or limitations of production systems and platforms. The contribution of the study enables the implementation of a reliable local change detection process. Supplementary processes can make use of this approach, such as updating and fusion of geospatial databases.

#### REFERENCES

- Ben-Haim, G., Dalyot, S., Doytsher, Y., 2014. Triangulation based topology approach for 2D point sets registration. *Survey Review*, 46(338), 355-365.
- Ben-Haim, G., Dalyot, S., Doytsher, Y., 2012. Localized accuracy assessment of topographic databases: ASTER case study. In *15th International Symposium on Spatial Data Handling*.
- Choussiafis, C., Karathanassi, V., Nikolakopoulos, K., 2012. Mosaic methods for improving the accuracy of interferometric based digital elevation models. In Perakis, K & Moysiadis, A. (Eds), *Proceedings of the 32nd EARSeL Symposium: Advances in Geosciences*, Greece.
- Dalyot, S., 2010. Hierarchical Modeling and Integration of Topographic Databases: Algorithm Development and Geo-Spatial Analysis Capabilities, Ph. D. Thesis. Technion, Haifa, Israel.
- Date, H., Kanai, S., Kishinami, T., 2001. An adaptive LOD Control Method for Textured Digital Terrain Model using Wavelet-based Multiresolution Representation. *Geoscience and Remote Sensing Symposium*, 4, 1847-1849.
- Falkowski, M. J., Smith, A. M., Hudak, A. T., Gessler, P. E., Vierling, L. A., & Crookston, N. L. (2006). Automated estimation of individual conifer tree height and crown diameter via two-dimensional spatial wavelet analysis of lidar data. *Canadian Journal of Remote Sensing*, 32(2), 153-161.
- Hebel, M., Arens, M., Stilla, U., 2013. Change detection in urban areas by object-based analysis and on-the-fly comparison of multi-view ALS data. *ISPRS Journal of Photogrammetry and Remote Sensing*, 86, 52- 64.
- Heipke, C., 2004. Some Requirements for Geographic Information Systems: A Photogrammetric Point of View, *Photogrammetric Engineering & Remote Sensing*, 70(2), 185- 195.
- Kršák, B., Blišťan, P., Pauliková, A., Puškárová, P., Kovanič, L., Palková, J., Zelizňaková, V., 2016. Use of low-cost UAV photogrammetry to analyze the accuracy of a digital elevation model in a case study. *Measurement*, 91, 276-287.
- Lowe, D. G., 1999. Object Recognition from Local Scale-Invariant Features. *Proceedings of the International Conference on Computer Vision*, 1150–1157.
- Lowe, D. G., 2004. Distinctive Image Features from Scale-Invariant keypoints. *International Journal on Computer Vision*. 2004, 91-110.
- Papasaika, H., Poli, D., Baltasvias, E., 2009. Fusion of Digital Elevation Models from Various Data Sources, *Int. Conf. on Advanced Geographic Inf. Systems & Web Services (GEOWS'09)*, 117–122.
- Papasaika, H., Kokiopoulou, E., Baltasvias, E., Schindler, K., Kressner, D., 2011. Fusion of Digital Elevation Models Using Sparse Representations, U. Stilla et al. (Eds.), *PIA 2011, LNCS 6952*, 171–184.
- Podobnikar, T., 2005. Production of integrated digital terrain model from multiple datasets of different quality. In: *Int. J. of Geographical Information Science*, 19(1), 69-89.
- Safra, E., Doytsher, Y., 2006. Using matching algorithms for improving locations in cadastral maps, *XXIII FIG Congress*, Munich, Germany, October 2006.
- Safra, E., Kanza, Y., Sagiv, Y., Doytsher, Y., 2006. Integrating Data from Maps on the World-Wide Web. In *Proc. of the 6th Int. Symp. on Web and Wireless Geographical Inf. Sys. (Springer)*, 180–191.
- Sester, M., Arsanjani, J.J., Klammer, R., Burghardt, D., Haunert, J.-H., 2014. Integrating and Generalising Volunteered Geographic Information Abstracting Geographic Information in a Data Rich World - Methodologies and Applications of Map Generalisation (119-155): Springer Heidelberg.
- Sharifi, M., Fathy, M., Mahmoudi, M.T., 2002. A classified and comparative study of edge detection algorithms. In *Proc. Int. Conf. on Inform. Technology: Coding and Computing*, Las Vegas, USA, 2002, 117-120.
- Tuttas, S., Braun, A., Borrmann, A., Stilla, U., 2017. Acquisition and consecutive registration of photogrammetric point clouds for construction progress monitoring using a 4D BIM. *PFJ-Journal of Photogrammetry, Remote Sensing and Geoinformation Science*, 85(1), 3-15
- Wang, Y., Wade, S.E., 2008. Comparisons of three types of DEMs: a case study of the Randleman reservoir, *N. Carolina. Southeastern Geographer*, 48(1), 110-124.
- Zhao, L., Yang, J., Li, P., Zhang, L., Shi, L., Lang, F., 2013. Damage assessment in urban areas using post-earthquake airborne PolSAR imagery. *International Journal of Remote Sensing*, 34, 8952–8966.